

# Epigenetic remodelling of gene expression profiles of neoplastic and normal tissues: immunotherapeutic implications

S Coral<sup>1,4</sup>, A Covre<sup>1,2,4</sup>, HJMG Nicolay<sup>1,2</sup>, G Parisi<sup>1,2</sup>, A Rizzo<sup>1</sup>, F Colizzi<sup>1</sup>, S Dalla Santa<sup>3</sup>, E Fonsatti<sup>2</sup>, E Fratta<sup>1</sup>, L Sigalotti<sup>1</sup> and M Maio<sup>\*,1,2</sup>

<sup>1</sup>Cancer Bioimmunotherapy Unit, Centro di Riferimento Oncologico, Istituto di Ricovero e Cura a Carattere Scientifico, Aviano, Italy; <sup>2</sup>Division of Medical Oncology and Immunotherapy, Department of Oncology, University Hospital of Siena, Istituto Toscano Tumori, Strada delle Scotte 14, 53100 Siena, Italy; <sup>3</sup>Department of Surgery, Oncology and Gastroenterology, Oncology and Immunology Division, University of Padua, Padua, Italy

**BACKGROUND:** Epigenetic remodelling of cancer cells is an attractive therapeutic strategy and distinct DNA hypomethylating agents (DHA) are being actively evaluated in patients with hemopoietic or solid tumours. However, no studies have investigated the modulation of gene expression profiles (GEP) induced by DHA in transformed and benign tissues. Such information is mandatory to clarify the fine molecular mechanism(s) underlying the clinical efficacy of DHA, to identify appropriate therapeutic combinations, and to address safety issues related to their demethylating potential in normal tissues. Thus, utilising a syngeneic mouse model, we investigated the remodelling of GEP of neoplastic and normal tissues induced by systemic administration of DHA.

**METHODS:** The murine mammary carcinoma cells TS/A were injected s.c. into female BALB/c mice that were treated i.p. with four cycles of the DHA 5-aza-2'-deoxycytidine (5-AZA-CdR) at a fractioned daily dose of 0.75 mg kg<sup>-1</sup> (q8 h × 3 days, every week). Whole mouse transcriptomes were analysed by microarrays in neoplastic and normal tissues from control and treated mice. Results were processed by bioinformatic analyses.

**RESULTS:** In all, 332 genes were significantly ( $P \leq 0.05$ ;  $FC \geq 4$ ) modulated (294 up and 38 downregulated) in neoplastic tissues from 5-AZA-CdR-treated mice compared with controls. In decreasing order of magnitude, changes in GEP significantly ( $P \leq 0.05$ ) affected immunologic, transport, signal transduction, spermatogenesis, and G-protein-coupled receptor protein signalling pathways. Epigenetic remodelling was essentially restricted to tumour tissues, leaving substantially unaltered normal ones.

**CONCLUSION:** The ability of 5-AZA-CdR to selectively target tumour GEP and its major impact on immune-related genes, strongly support the clinical use of DHA alone or combined with immunotherapeutic agents.

*British Journal of Cancer* (2012) **107**, 1116–1124. doi:10.1038/bjc.2012.361 www.bjcancer.com

Published online 21 August 2012

© 2012 Cancer Research UK

**Keywords:** DNA hypomethylation; gene expression profiling; 5-aza-2'-deoxycytidine; cancer; immunotherapy

Pharmacological DNA hypomethylation is an appealing strategy for cancer treatment owing to its pleiotropic activities that are only partially characterised. Among these, we have generated *in vitro* and *in vivo* evidences on the immunomodulatory activity of the DNA hypomethylating agent (DHA) 5-aza-2'-deoxycytidine (5-AZA-CdR) (Sigalotti *et al*, 2007). Exposure of different neoplastic cells to 5-AZA-CdR modulated their constitutive expression of HLA class I antigens, accessory/co-stimulatory molecules, and of different tumour-associated antigens, with particular relevance to cancer testis antigens (CTA) (Coral *et al*, 1999, 2002; Calabro *et al*, 2005; Coral *et al*, 2006, 2007; Fonsatti *et al*, 2007; Sigalotti *et al*, 2010). Of prospective clinical relevance, these phenotypic changes were shown: (i) to significantly improve the recognition of cancer cells by antigen-specific cytotoxic T lymphocytes (CTL) (Coral *et al*, 2006; Fonsatti *et al*, 2007); (ii) to abrogate the intratumoural heterogeneity of CTA expression by neoplastic cells, thus allowing for their homogeneous CTL recognition (Sigalotti *et al*, 2004); (iii) to increase the immunogenicity of transformed cells (Coral *et al*,

2006). These findings, altogether, identified 5-AZA-CdR as the 'prototype' DHA to be utilised in cancer patients; noteworthy, other DHA with a consistent immunological potential are also being developed (Coral *et al*, 2010).

Further supporting the foreseeable clinical immunomodulatory role of DHA, systemic administration of low-dose 5-AZA-CdR induced a persistent *de novo* expression of the CTA MAGE-A1, SSX 1-5, and NY-ESO-1 in peripheral blood and bone marrow mononuclear neoplastic cells of patients with acute myeloid leukaemia or myelodysplastic syndrome (Sigalotti *et al*, 2003), and of MAGE-A3 and NY-ESO-1 in tumour biopsies from patients with thoracic malignancies (Schrumpp *et al*, 2006). These phenotypic changes associated with the development of a humoral immune response against NY-ESO-1 in selected individuals (Schrumpp *et al*, 2006).

Despite these intriguing, highly appealing, results derived from the analysis of distinct immune molecules, no data are available on the more comprehensive modulation of tumour phenotypic profiles by *in vivo* administration of DHA, which might add relevance to their clinical effectiveness. Along this line, an additional issue that has not been addressed yet concerns the global effect(s) that DHA administration might have on the phenotypic profile of normal tissues; this aspect is of particular

\*Correspondence: Dr M Maio; E-mail: mmaio@cro.it

<sup>4</sup>These authors contributed equally to this work

Received 31 May 2012; revised 4 July 2012; accepted 17 July 2012; published online 21 August 2012

relevance to address safety concerns related to the use of DHA as immunomodulating agents.

Based on these evidences, we utilised a well-characterised/established experimental model, of s.c. injected cancer cells in mouse (Coral *et al*, 2006), to extensively evaluate the global effects of *in vivo* 5-AZA-CdR administration on both neoplastic and normal cells, by investigating changes in their gene expression profiles (GEP). In particular, we choose to s.c. inject, into the flank region of BALB/c mice, the poorly immunogenic murine mammary adenocarcinoma TS/A cells. While not being an orthotopic model, it has been described to represent a reliable system to pre-clinically validate immunological anti-tumour strategies potentially applicable to clinical settings (Rosato *et al*, 2003). We specifically focused on the effects of low doses of 5-AZA-CdR that have shown the most promising therapeutic activity in initial clinical trials in cancer patients (Daskalakis *et al*, 2010).

Epigenetic remodelling induced by *in vivo* 5-AZA-CdR resulted in a modified GEP of cancer cells mainly associated to immune processes. These modifications were preferentially found in tumour tissues, leaving normal ones essentially unaffected. The results presented in this study provide a comprehensive analysis of the *in vivo* epigenetic activity of DHA and greatly support the safety of their clinical use in cancer management, especially in combination with upcoming immunotherapeutic approaches.

## MATERIALS AND METHODS

### Reagents, cells and animals

5-AZA-CdR was purchased from Sigma Chemical Co. (St Louis, MO, USA).

The murine mammary carcinoma cells TS/A were cultured in DMEM as described (Nanni *et al*, 1983).

Six-week-old female BALB/c mice were obtained from Harlan Italy (Udine, Italy). Animal care and use were in accordance with the Institutional guidelines and the indications of Workman *et al* (2010).

### Mice treatment with 5-AZA-CdR

To obtain tumour cells engraftments, BALB/c mice were s.c. injected in the flank region with TS/A cells ( $2 \times 10^5$ ) suspended in 0.1 ml of physiologic saline. Animals were examined daily, and after a latency period of 1 week, mice bearing clearly palpable and visible tumour grafts were i.p. injected with four cycles of 5-AZA-CdR  $0.75 \text{ mg kg}^{-1}$ , in 0.2 ml of physiologic saline, fractionated every 8 h, for 3 days at weekly intervals, according to our previously defined schedule (5-AZA-CdR-treated mice) (Coral *et al*, 2006). Control mice were i.p. injected with 0.2 ml of physiologic saline. A week after the end of treatment, animals were killed by CO<sub>2</sub> overdose. Normal and neoplastic tissues were surgically removed and each sample was divided, under sterile conditions, to be frozen and used for RNA extraction.

### Whole genome transcriptome analysis

Total RNA extraction from tumour, spleen, and kidney specimens, excised from control mice and 5-AZA-CdR-treated mice, was performed as described (Coral *et al*, 1999). Spleen and kidney were selected as representative samples of hemopoietic and solid normal tissues, respectively, in light of their ability to provide sufficient amounts of total RNA. The quantity and the quality of RNA were assessed with NanoDrop ND-1000 UV-vis spectrophotometer (NanoDrop Technologies, Wilmington, DE, USA) and Agilent 2100 bioanalyzer (Agilent Technologies, Santa Clara, CA, USA). Total RNA was retrotranscribed to complementary DNA (cDNA) and complementary RNA (cRNA) was synthesised, amplified,

Cy3-labelled, and purified using the Quick Amp Labelling Kit, one-colour (Agilent Technologies) and the RNeasy Mini Kit (Qiagen, Milan, Italy), following manufacturers' guidelines. A mixture of 1650 ng of Cy3-labelled cRNA, Blocking Agent and Fragmentation Agent was hybridised to Whole Mouse Genome ( $4 \times 44 \text{ K}$ ) oligo microarray platform (Agilent Technologies). Hybridisation was performed for 17 h following Agilent recommendations. Following washing, tiff images were acquired from slides by Agilent Microarray Scanner. Data were extracted from tiff images by Feature Extraction Software (version 9.5.3) (Agilent).

### Bioinformatic analysis of global gene expression

Bioinformatic analyses were performed using GeneSpring GX 10.3. To determine which genes were differentially expressed between control and 5-AZA-CdR-treated mice, a two-sample unpaired Student's *t*-test, with Benjamini-Hochberg correction was utilised. For this analysis, genes with *P*-values  $\leq 0.05$  were considered statistically significant.

Genes identified as differentially expressed following 5-AZA-CdR treatment were evaluated for enrichment of Gene Ontology (GO) terms (Ashburner *et al*, 2000), considering biological process, utilising the Onto-Express web-tool (Draghici *et al*, 2003).

Gene Ontology terms were assigned to each sequence id based on its Entrez gene id. The final sets of GO terms were ranked based on their *P*-value. Gene Ontology terms were selected based on *P*-value  $\leq 0.05$  and on the number of associated genes ( $n \geq 5$ ).

### Reverse transcription (RT)-PCR analysis

To validate gene expression data, RT-PCR reactions were performed on six 5-AZA-CdR-treated mice and on six control animals as described (Coral *et al*, 1999). The Trap1a (P1A)- and Mage-a-specific oligonucleotide primer sequences and gene-specific PCR amplification programs used have been previously defined (Guo *et al*, 2006) (De Plaen *et al*, 1999). The integrity of each RNA and oligodeoxythymidine-synthesised cDNA samples was confirmed by the amplification of the mouse  $\beta$ -actin housekeeping gene, using sense mouse  $\beta$ -actin primer (5'-CCTTCTGGGCATGGAGTCT-3') and antisense mouse  $\beta$ -actin primer (5'-GGAGCAATGATCTTGATCTTC-3'). Ten microliters of each RT-PCR sample were run on a 2% agarose gel and visualised by ethidium bromide staining.

### Real-time quantitative RT-PCR analysis

Real-time quantitative RT-PCR analyses were performed as described (Calabro *et al*, 2005). Briefly, total RNA was digested with RNase-free DNase (Roche Diagnostics, Milan, Italy) to remove contaminating genomic DNA. Synthesis of cDNA was performed on 1  $\mu\text{g}$  total RNA using MMLV reverse transcriptase (Invitrogen, Milan, Italy) and random hexamer primers (Promega, Milan, Italy), following manufacturers' instructions. Measurement of gene expression was performed utilising the ABI prism 7000 Sequence Detection System (Applied Biosystems, Milan, Italy), as previously described (Calabro *et al*, 2005). Complementary DNA standards were obtained by RT-PCR amplification of the specific mRNAs and quantitated by NanoDrop ND-1000 UV-vis spectrophotometer. SYBR Green quantitative RT-PCR reactions were performed on 20 ng retrotranscribed total RNA in a final volume of 25  $\mu\text{l}$   $1 \times$  SYBR Green Master Mix (Applied Biosystems). The primers utilised for real-time RT-PCR assays were: P1A, forward 5'-GGTGCCGGAGCTGAGGA-3' and reverse 5'-TAGACACCAG-GAAATTAGGGTCG-3'; mouse  $\beta$ -actin, forward 5'-ACCAGTTCGC CATGGATGAC-3' and reverse 5'-TGCCGGAGCCGTTGTC-3'. The copy numbers of P1A and of the reference gene  $\beta$ -actin were established in each sample by extrapolation of the standard curve. The number of P1A cDNA molecules in each sample was then

normalised to the number of cDNA molecules of  $\beta$ -actin. The additional primer and probe sets utilised to further validate changes observed in GEP of cancer cells were chosen from TaqMan Gene Expression Assays designed by Applied Biosystems (i.e., *Spag16*, Assay ID Mm01256257\_m1; *H2-Q8*, Assay ID Mm02394722\_gH; *H2-K1*, Assay ID Mm01612247\_mH; *Ifih1*, Assay ID Mm00459183\_m1; *Psmb8*, Assay ID Mm00440207\_m1; *Psmb9*, Assay ID Mm00479004\_m1; *Tap1*, Assay ID Mm00443188\_m1; *Mage-a1*, Assay ID Mm04203946\_gH; *Mage-a6*, Assay ID Mm00522301\_s1; *Mage-a8*, Assay ID Mm00834740\_sH; *Pcdhb21*, Assay ID Mm00474621\_s1). Relative quantification of gene-specific mRNA was performed with the aid of the DataAssist v2.0 software (Applied Biosystems), using the  $\beta$ -actin housekeeping gene as endogenous control (Sigalotti *et al*, 2011).

Data were analysed by Student's paired *t*-test to identify significant differences between levels of investigated murine antigens induced by *in vivo* 5-AZA-CdR administration.

Pearson's product-moment correlation was evaluated between mean values of fold changes, induced by 5-AZA-CdR in the constitutive expression of selected genes, measured by microarray and quantitative RT-PCR analyses. The statistical analyses were performed using the R statistical environment (<http://www.R-project.org>).

### Quantitative methylation-specific PCR (qMSP) analyses

Genomic DNA was extracted from neoplastic tissues from untreated and 5-AZA-CdR-treated mice by proteinase K treatment followed by standard phenol/chloroform extraction and ethanol precipitation (Ausubel *et al*, 1998). Bisulfite conversion was carried out on 500 ng genomic DNA using EZ DNA Methylation-Gold Kit (Zymo Research, Orange, CA, USA), according to the manufacturer's protocol. Primers for the analysis of the methylation status of P1A were designed using the free online software MethPrimer (Li and Dahiya, 2002) and are: P1A (methylated), forward 5'-TTAA GTGCGTTATTACGTTTGGTTTTTAC-3', reverse 5'-ATAACCGAT TATTTAATACAAAAATCGACG-3'; P1A (unmethylated), forward 5'-GATTAAGTGTGTTATTATTGTTGGTTTTTAT-3', reverse 5'-A CATAACCAATTATTTAATACAAAAATCAACA-3'. SYBR green qMSP reactions were performed on 2  $\mu$ l of bisulfite-modified genomic DNA in a final volume of 25  $\mu$ l 1  $\times$  Power SYBR green Master Mix (Applied Biosystems) at 95  $^{\circ}$ C for 10 min, followed by 45 cycles of 15 s at 95  $^{\circ}$ C and 1 min at 60  $^{\circ}$ C, using methylated- or unmethylated-specific primer pairs. The copy number of methylated or unmethylated sequences for the target gene was established in each sample by extrapolation from the standard curves. The percentage of methylation was defined as the ratio between methylated molecules and the sum of methylated and unmethylated molecules.

### *In vitro* treatment of TS/A cells with 5-AZA-CdR

Cells were seeded at a density of  $3\text{--}4 \times 10^5$  cells in a T75 tissue culture flask and treated 24 h later with 5-AZA-CdR by replacing the medium with fresh medium, containing 1  $\mu$ M 5-AZA-CdR, every 12 h for 2 days (4 pulses) and then with fresh medium without 5-AZA-CdR for additional 2 days. Control cultures were treated under similar experimental conditions in the absence of 5-AZA-CdR. Cells were then processed for phenotypic and functional assays.

### Flow cytometric analysis

Indirect immunofluorescence analysis was done as previously described (Coral *et al*, 1999). The FITC-conjugated anti-MHC class I monoclonal antibody (mAb) MCA2189F was purchased from Serotec (Dusseldorf, Germany), the FITC-conjugated anti-MHC class I H-2D<sup>d</sup> from Abcam (Cambridge, UK), and the FITC-conjugated

anti-MHC class I H-2L<sup>d</sup> mAb from Acris Antibodies GmbH (Herford, Germany). A sample was classified as positive when more than 10% of cells were stained with the relevant mAb.

### Chromium release assay

Cytolytic activity was measured as described elsewhere utilising anti-P1A H-2L<sup>d</sup>-restricted CTL (Rosato *et al*, 2006). Briefly, <sup>51</sup>Cr-labelled target cells were incubated with effector cells at various E/T ratios in 96-well Falcon microplates. After 4 h of incubation at 37  $^{\circ}$ C, supernatants were harvested, and radioactivity was counted in a microplate scintillation counter (Top-Count; Packard Instruments, Meriden, CT, USA). For peptide pulsing, <sup>51</sup>Cr-labelled target cells (10<sup>6</sup> per ml) were incubated with the MHC class I L<sup>d</sup>-restricted peptide, corresponding to amino acids 35–43 of P1A protein, at 1  $\mu$ M final concentration, for 30 min at 37  $^{\circ}$ C and then washed twice before use. Cytotoxicity was expressed as per cent of lysis.

## RESULTS

### Modulation of GEP of neoplastic and normal tissues by 5-AZA-CdR

To characterise changes in GEP of cells from neoplastic and normal tissues following *in vivo* administration of 5-AZA-CdR, TS/A mammary carcinoma grafts and normal spleen and kidney tissues, excised from control and 5-AZA-CdR-treated mice, were analysed by whole mouse genome oligonucleotide microarrays. Spleen and kidney were selected as representative samples of hemopoietic and solid normal tissues, respectively.

5-AZA-CdR significantly ( $P \leq 0.05$ ) modulated the expression of 332 genes, with a  $FC \geq 4$ , in neoplastic tissues from 5-AZA-CdR-treated as compared with control mice. Among modulated genes, 38 were downregulated and 294 were upregulated (Supplementary Table S1).

To elucidate the biological significance of the genes representing the expression signature of 5-AZA-CdR-treated tumours, the gene identifiers for the 332 modulated genes were linked to the 'Onto-Express' web-based bioinformatic tool for global analysis of their function (Draghici *et al*, 2003). As summarised in Figure 1, and more in detail in Table 1, among the highest-scoring GO terms (considering  $P \leq 0.05$  and number of associated genes  $\geq 5$ ) are: (i) immune response (18 genes upregulated and 1 downregulated); (ii) transport (14 genes upregulated and 2 downregulated); (iii) signal transduction (10 genes upregulated and 2 downregulated); (iv) spermatogenesis (7 genes upregulated and 1 downregulated); (v) G-protein-coupled receptor protein signalling pathway (4 genes upregulated and 2 downregulated); (vi) antigen processing and presentation (all 5 genes upregulated); (vii) defence response to bacterium (all 5 genes upregulated); (viii) innate immune response (all 5 genes upregulated); and (ix) response to virus (all 5 genes upregulated).

Noteworthy, the gene expression signature of 5-AZA-CdR-treated tumours included the upregulated expression of several murine CTA (i.e., P1A and *Mage-a1*, *-a3*, *-a6*, *-a8*) (Supplementary Table S1), which are well-known as immune-related genes but are not included in the immunologic GO bioprocesses classes yet.

These major changes observed in GEP of tumour samples were not paralleled by similar modifications in GEP of normal tissues. Though, global analysis through the comparison of transcriptomes, identified 1020, 251, and 39 genes that were modulated, with a  $FC \geq 4$ , in tumour, spleen, and kidney samples, respectively, from 5-AZA-CdR-treated mice, as compared with tissues from control mice (data not shown). A Venn diagram was constructed illustrating the degree of overlap among genes modulated by 5-AZA-CdR, in the tissues under investigation (Figure 2).



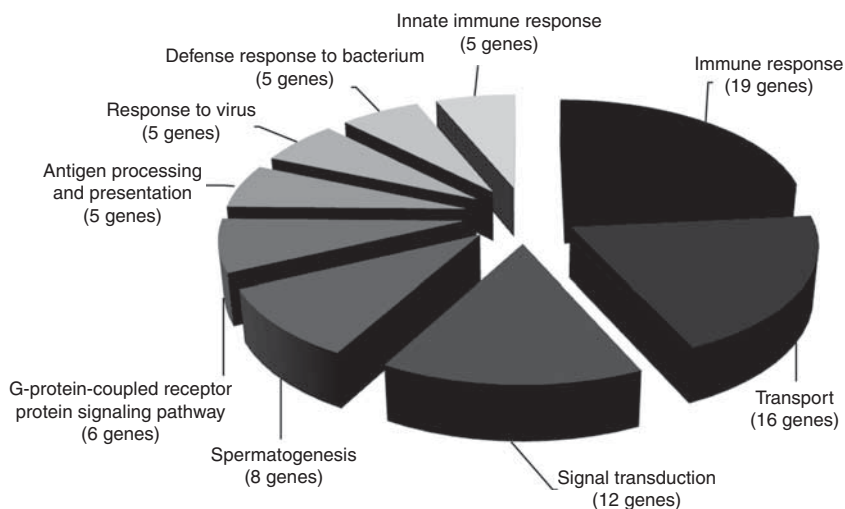


**Figure 1** Over-represented GO associated to the expression signature of 5-AZA-CdR-treated tumours. The gene identifier for the 332 genes, significantly modulated ( $P \leq 0.05$  and  $FC \geq 4$ ) in murine neoplastic grafts from 5-AZA-CdR-treated mice ( $n = 3$ ), as compared with control mice ( $n = 3$ ), were linked to the 'Onto-Express' web-based bioinformatic tool for global analysis of their function. Pie chart indicates the most over-represented GO terms, considering  $P \leq 0.05$  and number of associated genes  $\geq 5$ ; the size is relative to the number of represented genes. In brackets is the number of modulated genes in the specified biological process.

Modulation of GEP was highly tissue-specific, as very little overlap among different tissues was observed. Indeed, only 2 modulated genes were in common among the three tissue types analysed, 3 genes overlapped between spleens and kidneys, 12 genes overlapped between tumour and kidney specimens, and 45 genes overlapped between tumours and spleens (Figure 2 and Supplementary Table S2).

#### Validation of GEP changes by 5-AZA-CdR

To validate the significant changes induced by 5-AZA-CdR in GEP of cancer cells, real-time RT-PCR assays were performed in neoplastic tissues, from control and 5-AZA-CdR-treated mice, to quantify the expression of 11 genes, randomly selected for their differential up-/downregulation by 5-AZA-CdR. These include the sperm-associated antigen 16 gene (*Spag16*), the immune-related genes *H2-Q8*, *H2-K1*, *Ifih1*, *Psmb8*, *Psmb9*, *Tap1*, the murine CTA *Mage-a1*, *Mage-a6*, *Mage-a8*, and the protocadherin beta 21 gene (*Pcdhb21*). Mean values of fold changes induced by 5-AZA-CdR in the constitutive levels of gene expression, measured by quantitative RT-PCR assays, were compared with the mean fold changes obtained by microarray analysis. As plotted in Figure 3, a strong linear correlation was proved between measurements obtained from quantitative RT-PCR and microarray analyses ( $R^2 = 0.99$ ;  $P < 0.0001$ ).

#### Changes in CTA profile of neoplastic vs normal tissues by 5-AZA-CdR

To validate the alterations identified in GEP of neoplastic vs normal tissues, we specifically focused on molecules involved in immune recognition of neoplastic cells analysing the expression of a panel of CTA. To this end, RT-PCR analyses for the expression of the murine CTA P1A and of different *Mage-a* family members (i.e., *Mage-a1*, -a2, -a3, -a5, -a6, and -a8) were performed on neoplastic and normal tissues (i.e., spleen, blood, bone marrow, heart, liver, lung, and kidney) from control and 5-AZA-CdR-treated mice. A strong *de novo* expression of P1A and *Mage-a* members (Figure 4) was observed in tumour tissues excised from 5-AZA-CdR-treated animals, in comparison to the CTA-negative phenotype of neoplastic tissues from control mice. Conversely, no CTA induction was observed in normal tissues from 5-AZA-CdR-treated mice (Figure 4), with the exception of P1A, which became

weakly detectable in selected spleen (five out of six), blood (three out of six), and bone marrow (five out of six) samples from treated mice (Figure 4). However, quantitative real-time RT-PCR assays showed that levels of P1A-specific mRNA induced following 5-AZA-CdR treatment were significantly ( $P \leq 0.05$ ) higher in tumours as compared with normal tissues, with neoplastic tissues expressing 6, 9, and 12 times the amount of P1A mRNA expressed in paired spleen, blood, and bone marrow samples, respectively (Figure 5).

#### Methylation changes of P1A promoter in tumour tissues by 5-AZA-CdR

The methylation of CpG dinucleotides located in the promoter region of P1A was evaluated in neoplastic tissues from untreated and 5-AZA-CdR-treated mice to investigate whether hypomethylation of antigen promoter is the molecular mechanism sustaining the induced expression of P1A following 5-AZA-CdR administration. A reduction in the constitutive methylation status of P1A promoter, changing from  $96.10 \pm 1.35\%$  to  $58.65 \pm 5.78\%$ , was observed in neoplastic tissues following DHA treatment, supporting the role of pharmacological hypomethylation in the induced P1A expression (Figure 6).

#### Functional role of changes by *in vitro* 5-AZA-CdR

To evaluate whether changes induced by 5-AZA-CdR on the immune profile of cancer cells could make them more sensitive to the host's immune recognition, TS/A cells were *in vitro* treated with  $1 \mu\text{M}$  5-AZA-CdR and tested by phenotypic and functional assays. Along this line, flow cytometric analysis demonstrated that *in vitro* exposure to 5-AZA-CdR upregulated the constitutive expression of MHC class I antigens and of the MHC haplotype antigens H-2D<sup>d</sup> and H-2L<sup>d</sup> (Figure 7A). Data obtained from a representative experiment demonstrated that values of mean fluorescence intensity for TS/A cells untreated or treated with 5-AZA-CdR were 30.63 and 64.05 for MHC class I, 31.44 and 121.95 for H-2D<sup>d</sup>, 32.45 and 63.39 for H-2L<sup>d</sup>, respectively (Figure 7A). At the same time, real-time RT-PCR analysis showed that the number of P1A-specific mRNA molecules in tumour cells went from  $1.46 \times 10^{-6}$  to  $5.24 \times 10^{-3}$ , following exposure to 5-AZA-CdR (data not shown).

**Table 1** Over-represented biological processes associated with *in vivo* modulation of tumour GEP by 5-AZA-CdR

Biological process	Gene symbol	Gene name	FC <sup>a</sup>
Immune response	<i>Crtam</i>	cytotoxic and regulatory T-cell molecule	22, 8
	<i>H2-Q8</i>	histocompatibility 2, Q region locus 8	17, 2
	<i>C2</i>	complement component 2 (within H-2S)	16, 9
	<i>Tgtp</i>	T-cell-specific GTPase	11, 0
	<i>Cxcl11</i>	chemokine (C-X-C motif) ligand 11	10, 1
	<i>Gbp3</i>	guanylate-binding protein 3	8, 1
	<i>Oasl2</i>	2'-5' oligoadenylate synthetase-like 2	6, 9
	<i>Psmb9</i>	proteasome (prosome, macropain) subunit, beta type 9 (large multifunctional peptidase 2)	6, 5
	<i>Gbp5</i>	guanylate-binding protein 5	6, 4
	<i>Gbp1</i>	guanylate-binding protein 1	6, 3
	<i>Serpina3g</i>	serine (or cysteine) peptidase inhibitor, clade A, member 3G	5, 9
	<i>Tap1</i>	transporter 1, ATP-binding cassette, sub-family B (MDR/TAP)	5, 8
	<i>Gbp2</i>	guanylate-binding protein 2	4, 7
	<i>H2-K1</i>	histocompatibility 2, K1, K region	4, 4
	<i>H2-Q9</i>	histocompatibility 2, Q region locus 9	4, 3
	<i>Iflh1</i>	interferon induced with helicase C domain 1	4, 3
	<i>Psmb8</i>	proteasome (prosome, macropain) subunit, beta type 8 (large multifunctional peptidase 7)	4, 3
	<i>Irgm</i>	immunity-related GTPase family M member 1	4, 1
	<i>Tnfrsf12</i>	tumour necrosis factor (ligand) superfamily, member 12	-9, 6
	Transport	<i>I300013J15Rik</i>	solute carrier family 47, member 1
<i>Rab3b</i>		RAB3B, member RAS oncogene family	132, 5
<i>Slc25a31</i>		solute carrier family 25 (mitochondrial carrier; adenine nucleotide translocator), member 31	63, 2
<i>Chma10</i>		cholinergic receptor, nicotinic, alpha polypeptide 10	28, 9
<i>Slc2a12</i>		solute carrier family 2 (facilitated glucose transporter), member 12	27, 7
<i>1190003J15Rik</i>		RIKEN complementary DNA 1190003J15 gene	25, 4
<i>Slc38a4</i>		solute carrier family 38, member 4	20, 0
<i>4933425K02Rik</i>		Na <sup>+</sup> /H <sup>+</sup> exchanger domain containing 1	16, 8
<i>AB182283</i>		NAC alpha domain containing	14, 5
Transport		<i>Gabrd</i>	gamma-aminobutyric acid (GABA) A receptor, subunit delta
	<i>Slc16a11</i>	solute carrier family 16 (monocarboxylic acid transporters), member 11	10, 5
	<i>Best3</i>	bestrophin 3	10, 2
	<i>Tap1</i>	transporter 1, ATP-binding cassette, sub-family B (MDR/TAP)	5, 8
	<i>Abcb9</i>	ATP-binding cassette, sub-family B (MDR/TAP), member 9	5, 0
	<i>9830002I17Rik</i>	spinster homologue 3 ( <i>Drosophila</i> )	-7, 5
<i>Abcg8</i>	ATP-binding cassette, sub-family G (WHITE), member 8	-5, 1	
Signal transduction	<i>Olfrl221</i>	olfactory receptor 1221	28, 7
	<i>Baiap211</i>	BAI1-associated protein 2-like 1	11, 0
	<i>Ccr1</i>	chemokine (C-C motif) receptor-like 1	8, 3
	<i>Il18r1</i>	interleukin 18 receptor 1	8, 3
	<i>Amhr2</i>	anti-Mullerian hormone type 2 receptor	6, 9
	<i>Wnt6</i>	wingless-related MMTV integration site 6	6, 6
	<i>Ptgfr</i>	prostaglandin F receptor	6, 2
	<i>Olfrl37</i>	olfactory receptor 137	5, 0
	<i>Amtl2</i>	aryl hydrocarbon receptor nuclear translocator-like 2	4, 8
	<i>Stat1</i>	signal transducer and activator of transcription 1	4, 4
	<i>Cx3cr1</i>	chemokine (C-X3-C) receptor 1	-4, 8
	<i>Ccr1</i>	chemokine (C-C motif) receptor 1	-6, 5
	Spermatogenesis	<i>Spag16</i>	sperm-associated antigen 16
<i>Dazl</i>		deleted in azoospermia-like	92, 2
<i>Taf7l</i>		TAF7-like RNA polymerase II, TATA box-binding protein (TBP)-associated factor	39, 9
<i>Pax5</i>		paired box gene 5	29, 2
<i>Sohlh2</i>		spermatogenesis and oogenesis-specific basic helix-loop-helix 2	26, 1
<i>Stra8</i>		stimulated by retinoic acid gene 8	8, 3
<i>Piwil2</i>		piwi-like homologue 2 ( <i>Drosophila</i> )	4, 8
<i>Bmp8a</i>		bone morphogenetic protein 8a	-7, 9
G-protein-coupled receptor protein signalling pathway	<i>Olfrl221</i>	olfactory receptor 1221	28, 7
	<i>Ccr1</i>	chemokine (C-C motif) receptor-like 1	8, 3
G-protein-coupled receptor protein signalling pathway	<i>Ptgfr</i>	prostaglandin F receptor	6, 2
	<i>Olfrl37</i>	olfactory receptor 137	5, 0
	<i>Cx3cr1</i>	chemokine (C-X3-C) receptor 1	-4, 8
	<i>Ccr1</i>	chemokine (C-C motif) receptor 1	-6, 5
Antigen processing and presentation	<i>H2-Q8</i>	histocompatibility 2, Q region locus 8	17, 2
	<i>Psmb9</i>	proteasome (prosome, macropain) subunit, beta type 9 (large multifunctional peptidase 2)	6, 5
	<i>H2-K1</i>	histocompatibility 2, K1, K region	4, 4
	<i>H2-Q9</i>	histocompatibility 2, Q region locus 9	4, 3
	<i>Psmb8</i>	proteasome (prosome, macropain) subunit, beta type 8 (large multifunctional peptidase 7)	4, 3
Defence response to bacterium	<i>Hamp2</i>	hepcidin antimicrobial peptide 2	167, 7
	<i>Wfdc15a</i>	WAP four-disulphide core domain 15A	83, 2
	<i>Nlrp1a</i>	NLR family, pyrin domain-containing 1A	8, 0
	<i>Ifnb1</i>	interferon beta 1, fibroblast	6, 0
	<i>H2-K1</i>	histocompatibility 2, K1, K region	4, 4

Table 1 (Continued)

Biological process	Gene symbol	Gene name	FC <sup>a</sup>
Innate immune response	<i>C2</i>	complement component 2 (within H-2S)	16.9
	<i>Il18r1</i>	interleukin 18 receptor 1	8.3
	<i>Mx2</i>	myxovirus (influenza virus) resistance 2	7.4
	<i>Irfh1</i>	interferon induced with helicase C domain 1	4.3
	<i>Irgm</i>	immunity-related GTPase family M member 1	4.1
Response to virus	<i>Tgtp</i>	T-cell-specific GTPase	11.0
	<i>Mx2</i>	myxovirus (influenza virus) resistance 2	7.4
	<i>Irfb1</i>	interferon beta 1, fibroblast	6.0
	<i>Irf7</i>	interferon regulatory factor 7	5.6
	<i>Irfh1</i>	interferon induced with helicase C domain 1	4.3

<sup>a</sup>FC indicates fold change of gene expression in tumour tissues from 5-AZA-CdR-treated vs control mice.

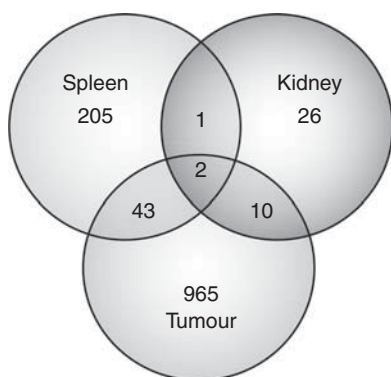


**Figure 2** Venn diagram of genes modulated by *in vivo* 5-AZA-CdR in tumour, spleen, and kidney tissues. Global analysis of the variation in GEP of the full dataset identified 1020, 251, and 39 genes, for which expression was, respectively, modulated ( $FC \geq 4$ ) in tumour, spleen, and kidney samples from 5-AZA-CdR-treated mice ( $n = 3$ ), as compared with tissues from control mice ( $n = 3$ ). Venn diagram illustrates the overlaps of genes modulated ( $FC \geq 4$ ) by the treatment among investigated tissues. For a detailed listing of all the genes in the overlaps, see Supplementary Table S2.

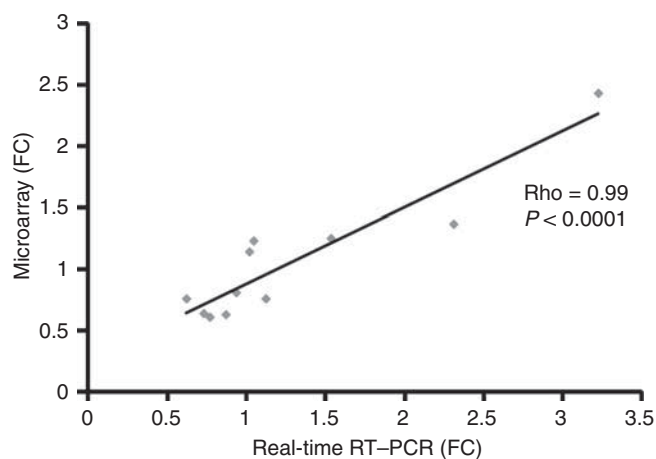


**Figure 3** Correlation among expression values from GEP and quantitative RT-PCR analyses. Quantitative real-time RT-PCR assays were performed in neoplastic tissues from control and 5-AZA-CdR-treated mice to quantify the expression of 11 selected genes (i.e., *Spag16*, *H2-Q8*, *H2-K1*, *Irfh1*, *Psm8*, *Psm9*, *Tap1*, *Mage-a1*, *Mage-a6*, *Mage-a8*, and *Pcdhb21*). Mean values of fold changes induced by 5-AZA-CdR in the constitutive levels of gene-specific mRNA expression were correlated to the mean GEP changes observed by the microarray analysis using Pearson's product-moment correlation. Data are reported on a logarithmic scale.

Based on these results, to evaluate whether modulation of the immune profile induced by 5-AZA-CdR was effective in increasing immune recognition of cancer cells, cytolytic activity of P1A-specific CTL was measured against TS/A untreated or *in vitro* treated with  $1 \mu\text{M}$  5-AZA-CdR, pulsed or not with P1A peptide. As evidenced in Figure 7B, the lytic activity of P1A-specific T cells was higher against 5-AZA-CdR-treated as compared with untreated TS/A cells, but it was measurable only against P1A-pulsed target cells. This observation could be explained by the absence of P1A expression at protein level, following 5-AZA-CdR exposure, as revealed by western blot analysis (Supplementary Figure 1).

## DISCUSSION

This work provides novel information on the global *in vivo* effects of DHA on the phenotypic profile of transformed and benign cells. Specifically, we demonstrated that the epigenetic activity of low-dose 5-AZA-CdR is highly effective in modifying the GEP of neoplastic cells, being particularly directed towards the modulation of their immune profile. Furthermore, the epigenetic remodelling of GEP was preferentially restricted to tumour tissues, leaving almost unaltered the phenotype of normal ones. Altogether, these findings further clarify the pleiotropic molecular *in vivo* effects of DHA and greatly enforce the scientific rationale in support of their therapeutic use as epigenetic immunomodulators for the treatment of human malignancies.

In cancer tissues, 5-AZA-CdR significantly modulated the expression of 332 genes involved in different biological processes. As expected, the genes with the highest upregulation were associated to gametogenesis and embryonic development (Supplementary Table S1) that are well known for their physiological epigenetic regulation (Kafri *et al*, 1992). Nevertheless, when data were analysed to identify the biological pathways affected by 5-AZA-CdR, immunological processes (i.e., immune response, tumour-antigen presentation, and immune recognition) turned out to be the most significantly modulated. A detailed analysis will be required to characterise the comprehensive immunological consequences of the preferential modulation of the immune signature of tumour cells by 5-AZA-CdR; however, the identified concomitant upregulation of MHC class I molecules and of different components of the antigen processing and presentation machinery (i.e., *Tap1*, *Psm8*, *Psm9*), together with the induction of different CTA (i.e., P1A and *Mage-a* family members), univocally directs neoplastic tissues towards a more targetable/immunogenic profile. This notion is supported by our *in vitro* evidences demonstrating that 5-AZA-CdR treatment results in an increased lysis of TS/A cells by P1A-specific CTL, which was at least in part sustained by the upregulation of MHC class I antigens (Figure 7). This functional effect became measurable only after pulsing of target cells with P1A peptide,

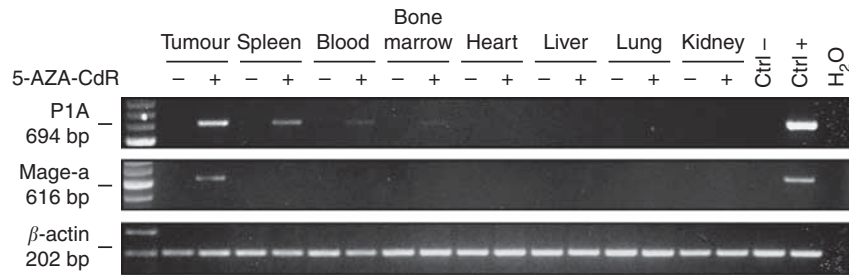


**Figure 4** Reverse transcription–PCR analysis of murine CTA expression in tumour and normal tissues (spleen, blood, bone marrow, heart, liver, lung, and kidney) of control (–) and 5-AZA-CdR-treated (+) mice. Total RNA was extracted from tumour and normal tissues (spleen, blood, bone marrow, heart, liver, lung, and kidney) of control (–) and 5-AZA-CdR-treated (+) mice. Total RNA from mouse splenocytes and testis was utilised as negative control (ctrl –) or positive control (ctrl +), respectively. Reverse transcription–PCR analysis was performed using P1A-, Mage-a- or β-actin-specific primer pairs. Polymerase chain reaction products were then separated on a 2% agarose gel and visualised by ethidium bromide staining. Figure shows data from one representative mouse out of six for both control and 5-AZA-CdR-treated groups.

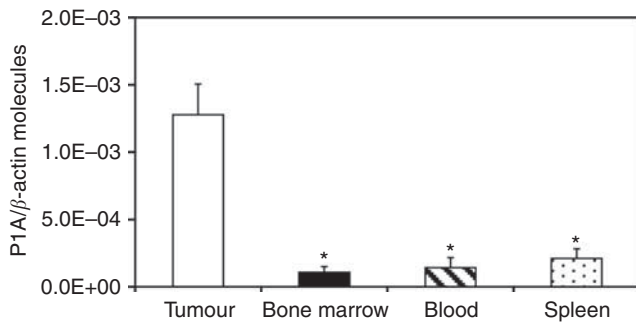


**Figure 5** Quantitative RT–PCR analysis of P1A expression in tumour and normal tissues from 5-AZA-CdR-treated mice. Total RNA was extracted from tumour, bone marrow, blood, and spleen samples from 5-AZA-CdR-treated mice. Retrotranscribed RNA was subjected to SYBR Green quantitative real-time RT–PCR analysis using P1A- and β-actin-specific primers. Data are reported as P1A molecules/β-actin molecules. Columns, mean values of P1A molecules/β-actin molecules from six distinct mice; bars, s.d.; \* $P \leq 0.05$  vs tumour samples.

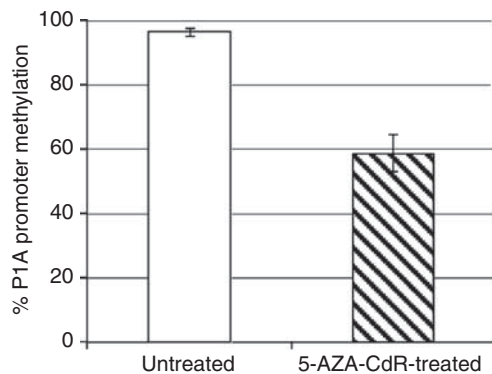


**Figure 6** Methylation status of P1A promoter in neoplastic tissues from untreated and 5-AZA-CdR-treated mice. Genomic DNA was extracted from neoplastic tissues from untreated (white column) or 5-AZA-CdR-treated (stripped column) mice and subjected to sodium bisulfite modification. Real-time qMSP analyses of P1A promoter were performed on bisulfite-modified genomic DNA using methylated- or unmethylated-specific primer pairs. Data are reported as percentage of methylation, defined as the ratio between methylated molecules and the sum of methylated and unmethylated molecules. Columns, mean values of the percentage of P1A promoter methylation from 3 distinct untreated or 5-AZA-CdR-treated mice; bars, s.d.

due to the lack of induction of P1A protein by demethylating treatment (Supplementary Figure S1). Whether the failure in producing P1A protein following 5-AZA-CdR depends on additional post-transcriptional requirements necessary in TS/A and/or other neoplastic cells is still unknown. This observation, however, is likely confined to the reported setting, as the ability of 5-AZA-CdR to induce the expression of CTA, efficiently recognised by CTA-specific CTL, is well characterised both in human and mouse cancer cells (Coral *et al*, 2002; Sigalotti *et al*, 2004; Guo *et al*, 2006). More importantly, the increased recognition of P1A-peptide pulsed TS/A cells following 5-AZA-CdR treatment sustains a broad immunomodulatory activity of epigenetic drugs, which grants their use for generally improving tumour immune recognition, both through methylation-regulated and non-methylation-regulated target antigens, as previously reported in human melanoma (Fonsatti *et al*, 2007).

From a translational clinical perspective, an additional finding of this study is that the modifications of GEP induced by 5-AZA-CdR, did not significantly affect normal tissues. This represents a key learning in light of the clinical use of DHA as immunomodulatory agents. In fact, by preferentially targeting the sole tumour cells, DHA should neither induce immune reaction(s) against normal tissues when utilised alone, nor increase that of immunotherapeutic agents (Di Giacomo *et al*, 2010; Fratta *et al*, 2011; Garbe *et al*, 2011) in combination strategies. The S-phase specificity of 5-AZA-CdR is likely at the base of this tumour-restricted activity of the drug, that efficiently targets the highly proliferating cancer cells as compared with the low-/non-replicating normal cells (Momparker, 1985). Further support to the limited activity of 5-AZA-CdR on normal tissues derives from the observation that *in vitro* PHA-activated and DHA-treated mouse splenocytes, though expressing high levels of P1A, were not tumorigenic once injected *i.p.* into nude mice (Coral and Maio, unpublished data).

Our present results obtained utilising low-dose 5-AZA-CdR, also contributes to address the still actively debated issue on the identification of its optimal schedule and dose of administration. Available data suggest that the anti-neoplastic activity of 5-AZA-CdR has a dose-dependent, dual mechanism of action: promoting cell death by cytotoxicity at high doses and inhibiting DNA methylation at low doses (Issa and Kantarjian, 2009). Despite the limited anti-tumour activity of low-dose 5-AZA-CdR, a portion of patients with solid tumours exhibited interesting immunological responses represented by the induction of CTA (i.e., MAGE-A3 and NY-ESO-1) in tumour biopsies, and by the development of circulating anti-NY-ESO-1 antibodies (Schrumpp *et al*, 2006). In this context, our demonstration that a low-dose schedule of 5-AZA-CdR preferentially modulates immunological pathways of tumour cells, leaving unaltered GEP of normal tissues, strongly



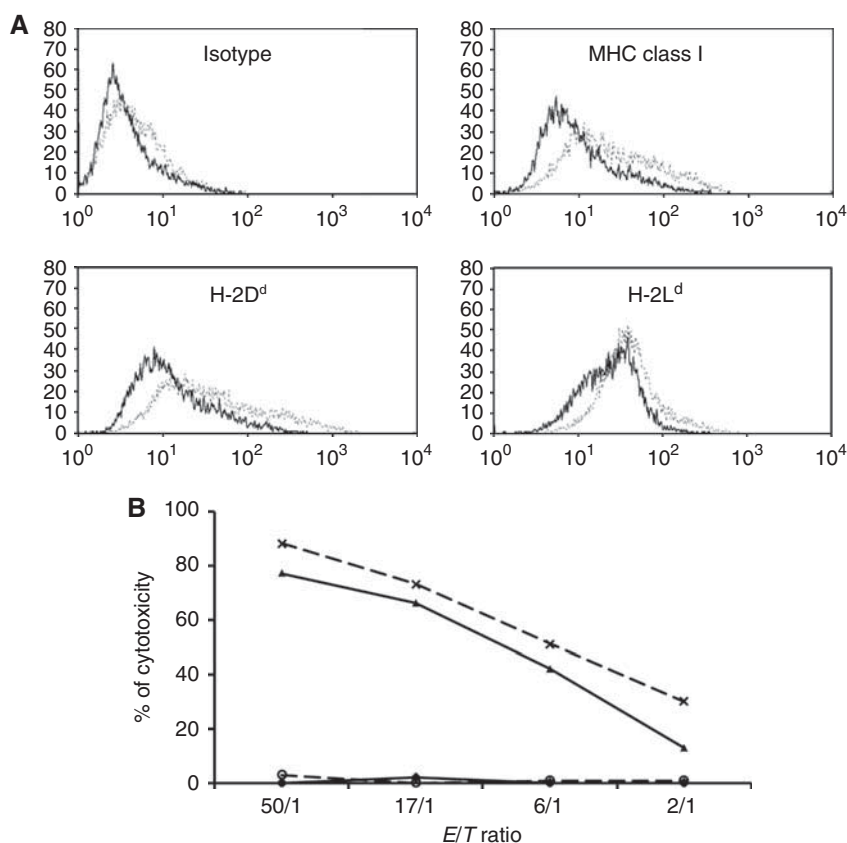


**Figure 7** Phenotypic and functional analyses of changes induced by *in vitro* 5-AZA-CdR. **(A)** TS/A cells either untreated (—), or treated with 1  $\mu$ M 5-AZA-CdR (- - -), were incubated with the FITC-conjugated anti-MHC class I, anti-H-2D<sup>d</sup>, or anti-H-2L<sup>d</sup> mAbs. Cells were then analysed by flow cytometry. **(B)** Cytolytic activity of anti-PIA H-2L<sup>d</sup>-restricted CTL was measured by chromium release assay against <sup>51</sup>Cr-labelled TS/A cells untreated (—) or treated (- - -) with 1  $\mu$ M 5-AZA-CdR every 12 h for 2 days, at effector/target (E/T) ratios of 50:1, 17:1, 6:1, and 2:1. For peptide pulsing, <sup>51</sup>Cr-labelled target cells (10<sup>6</sup> per ml) were incubated with the MHC class I L<sup>d</sup>-restricted peptide corresponding to amino acids 35–43 of PIA protein, at 1  $\mu$ M final concentration, for 30 min at 37 °C, and then washed twice before use (crossed squares and triangle points). Cytotoxicity was expressed as per cent of lysis. Data reported are representative of three independent experiments.

supports the clinical use of non-cytotoxic doses of DHA as immunomodulatory agents.

Overall, our present results provide a strong scientific rationale to implement novel anti-cancer therapeutic strategies contemplating their use as immunomodulators. Along this line, particular emphasis should be devoted to combination strategies with active and/or adoptive immunotherapeutic approaches that target specific tumour antigens on neoplastic cells. Nevertheless, the broad immunomodulatory activity of DHA will undoubtedly allow to extend their use also in combination with non-specific immunotherapeutic strategies, such as immunomodulating antibodies (Boasberg *et al*, 2010) that are emerging as powerful therapeutic tools in solid tumours of different histotypes (Calabro *et al*, 2010; Robert *et al*, 2011).

## REFERENCES

- Ashburner M, Ball CA, Blake JA, Botstein D, Butler H, Cherry JM, Davis AP, Dolinski K, Dwight SS, Eppig JT, Harris MA, Hill DP, Issel-Tarver L, Kasarskis A, Lewis S, Matese JC, Richardson JE, Ringwald M, Rubin GM, Sherlock G (2000) Gene ontology: tool for the unification of biology. The Gene Ontology Consortium. *Nat Genet* 25(1): 25–29
- Ausubel FM, Brent R, Kingston RE (1998) *Current Protocols in Molecular Biology*. John Wiley & Sons: New York
- Boasberg P, Hamid O, O'Day S (2010) Ipilimumab: unleashing the power of the immune system through CTLA-4 blockade. *Semin Oncol* 37(5): 440–449

## ACKNOWLEDGEMENTS

This work was supported in part by grants from Associazione Italiana per la Ricerca sul Cancro (IG 6038 to MM and MFAG 9195 to LS), Harry J Lloyd Charitable Trust (MM), Istituto Superiore di Sanità (MM), Istituto Toscano Tumori (MM) and Monte dei Paschi di Siena (SC).

## Conflict of interest

The authors declare no conflict of interest.

Supplementary Information accompanies the paper on British Journal of Cancer website (<http://www.nature.com/bjc>)

- Calabro L, Danielli R, Sigalotti L, Maio M (2010) Clinical studies with anti-CTLA-4 antibodies in non-melanoma indications. *Semin Oncol* 37(5): 460–467
- Calabro L, Fonsatti E, Altomonte M, Pezzani L, Colizzi F, Nanni P, Gattei V, Sigalotti L, Maio M (2005) Methylation-regulated expression of cancer testis antigens in primary effusion lymphoma: immunotherapeutic implications. *J Cell Physiol* 202(2): 474–477
- Coral S, Sigalotti L, Altomonte M, Engelsberg A, Colizzi F, Cattarossi I, Maraskovsky E, Jager E, Seliger B, Maio M (2002) 5-aza-2'-deoxycytidine-induced expression of functional cancer testis antigens in human



- renal cell carcinoma: immunotherapeutic implications. *Clin Cancer Res* 8(8): 2690–2695
- Coral S, Sigalotti L, Colizzi F, Spessotto A, Nardi G, Cortini E, Pezzani L, Fratta E, Fonsatti E, Di Giacomo AM, Nicotra MR, Natali PG, Altomonte M, Maio M (2006) Phenotypic and functional changes of human melanoma xenografts induced by DNA hypomethylation: immunotherapeutic implications. *J Cell Physiol* 207(1): 58–66
- Coral S, Sigalotti L, Covre A, Nicolay HJ, Natali PG, Maio M (2007) 5-AZA-2'-deoxycytidine in cancer immunotherapy: a mouse to man story. *Cancer Res* 67(6): 2900–2901 (author reply 2901–2902)
- Coral S, Sigalotti L, Fonsatti E, Parisi G, Colizzi F, Nicolay HJ, Taverna P, Maio M (2010) Immunobiologic activity of the demethylating dinucleotide SGI-110. *J Immunother* 33(8): 893–894
- Coral S, Sigalotti L, Gasparollo A, Cattarossi I, Visintin A, Cattelan A, Altomonte M, Maio M (1999) Prolonged upregulation of the expression of HLA class I antigens and costimulatory molecules on melanoma cells treated with 5-aza-2'-deoxycytidine (5-AZA-CdR). *J Immunother* 22(1): 16–24
- Daskalakis M, Blagitko-Dorfs N, Hackanson B (2010) Decitabine. *Recent Results Cancer Res* 184: 131–157
- De Plaen E, De Backer O, Arnaud D, Bonjean B, Chomez P, Martelange V, Avner P, Baldacci P, Babinet C, Hwang SY, Knowles B, Boon T (1999) A new family of mouse genes homologous to the human MAGE genes. *Genomics* 55(2): 176–184
- Di Giacomo AM, Biagioli M, Maio M (2010) The emerging toxicity profiles of anti-CTLA-4 antibodies across clinical indications. *Semin Oncol* 37(5): 499–507
- Draghici S, Khatri P, Bhavsar P, Shah A, Krawetz SA, Tainsky MA (2003) Onto-Tools, the toolkit of the modern biologist: Onto-Express, Onto-Compare, Onto-Design and Onto-Translate. *Nucleic Acids Res* 31(13): 3775–3781
- Fonsatti E, Nicolay HJ, Sigalotti L, Calabro L, Pezzani L, Colizzi F, Altomonte M, Guidoboni M, Marincola FM, Maio M (2007) Functional up-regulation of human leukocyte antigen class I antigens expression by 5-aza-2'-deoxycytidine in cutaneous melanoma: immunotherapeutic implications. *Clin Cancer Res* 13(11): 3333–3338
- Fratta E, Coral S, Covre A, Parisi G, Colizzi F, Danielli R, Marie Nicolay HJ, Sigalotti L, Maio M (2011) The biology of cancer testis antigens: putative function, regulation and therapeutic potential. *Mol Oncol* 5(2): 164–182
- Garbe C, Eigentler TK, Keilholz U, Hauschild A, Kirkwood JM (2011) Systematic review of medical treatment in melanoma: current status and future prospects. *Oncologist* 16(1): 5–24
- Guo ZS, Hong JA, Irvine KR, Chen GA, Spiess PJ, Liu Y, Zeng G, Wunderlich JR, Nguyen DM, Restifo NP, Schrum DS (2006) *De novo* induction of a cancer/testis antigen by 5-aza-2'-deoxycytidine augments adoptive immunotherapy in a murine tumor model. *Cancer Res* 66(2): 1105–1113
- Issa JP, Kantarjian HM (2009) Targeting DNA methylation. *Clin Cancer Res* 15(12): 3938–3946
- Kafri T, Ariel M, Brandeis M, Shemer R, Urven L, McCarrey J, Cedar H, Razin A (1992) Developmental pattern of gene-specific DNA methylation in the mouse embryo and germ line. *Genes Dev* 6(5): 705–714
- Li LC, Dahiya R (2002) MethPrimer: designing primers for methylation PCRs. *Bioinformatics* 18(11): 1427–1431
- Momparler RL (1985) Molecular, cellular and animal pharmacology of 5-aza-2'-deoxycytidine. *Pharmacol Ther* 30(3): 287–299
- Nanni P, de Giovanni C, Lollini PL, Nicoletti G, Prodi G (1983) TS/A: a new metastasizing cell line from a BALB/c spontaneous mammary adenocarcinoma. *Clin Exp Metastasis* 1(4): 373–380
- Robert C, Thomas L, Bondarenko I, O'Day S, Weber J, Garbe C, Lebbe C, Baurain JF, Testori A, Grob JJ, Davidson N, Richards J, Maio M, Hauschild A, Miller Jr WH, Gascon P, Lotem M, Harmankaya K, Ibrahim R, Francis S, Chen TT, Humphrey R, Hoos A, Wolchok JD (2011) Ipilimumab plus dacarbazine for previously untreated metastatic melanoma. *N Engl J Med* 364(26): 2517–2526
- Rosato A, Dalla Santa S, Zoso A, Giacomelli S, Milan G, Macino B, Tosello V, Dellabona P, Lollini PL, De Giovanni C, Zanovello P (2003) The cytotoxic T-lymphocyte response against a poorly immunogenic mammary adenocarcinoma is focused on a single immunodominant class I epitope derived from the gp70 Env product of an endogenous retrovirus. *Cancer Res* 63(9): 2158–2163
- Rosato A, Zoso A, Dalla Santa S, Milan G, Del Bianco P, De Salvo GL, Zanovello P (2006) Predicting tumor outcome following cancer vaccination by monitoring quantitative and qualitative CD8+ T cell parameters. *J Immunol* 176(3): 1999–2006
- Schrump DS, Fischette MR, Nguyen DM, Zhao M, Li X, Kunst TF, Hancox A, Hong JA, Chen GA, Pishchik V, Figg WD, Murgo AJ, Steinberg SM (2006) Phase I study of decitabine-mediated gene expression in patients with cancers involving the lungs, esophagus, or pleura. *Clin Cancer Res* 12(19): 5777–5785
- Sigalotti L, Altomonte M, Colizzi F, Degan M, Rupolo M, Zagonel V, Pinto A, Gattei V, Maio M (2003) 5-Aza-2'-deoxycytidine (decitabine) treatment of hematopoietic malignancies: a multimechanism therapeutic approach? *Blood* 101(11): 4644–4646
- Sigalotti L, Covre A, Fratta E, Parisi G, Colizzi F, Rizzo A, Danielli R, Nicolay HJ, Coral S, Maio M (2010) Epigenetics of human cutaneous melanoma: setting the stage for new therapeutic strategies. *J Transl Med* 8: 56
- Sigalotti L, Fratta E, Bidoli E, Covre A, Parisi G, Colizzi F, Coral S, Massarut S, Kirkwood JM, Maio M (2011) Methylation levels of the 'long interspersed nucleotide element-1' repetitive sequences predict survival of melanoma patients. *J Transl Med* 9: 78
- Sigalotti L, Fratta E, Coral S, Cortini E, Covre A, Nicolay HJ, Anzalone L, Pezzani L, Di Giacomo AM, Fonsatti E, Colizzi F, Altomonte M, Calabro L, Maio M (2007) Epigenetic drugs as pleiotropic agents in cancer treatment: biomolecular aspects and clinical applications. *J Cell Physiol* 212(2): 330–344
- Sigalotti L, Fratta E, Coral S, Tanzarella S, Danielli R, Colizzi F, Fonsatti E, Traversari C, Altomonte M, Maio M (2004) Intratumor heterogeneity of cancer/testis antigens expression in human cutaneous melanoma is methylation-regulated and functionally reverted by 5-aza-2'-deoxycytidine. *Cancer Res* 64(24): 9167–9171
- Workman P, Aboagye EO, Balkwill F, Balmain A, Bruder G, Chaplin DJ, Double JA, Everitt J, Farningham DA, Glennie MJ, Kelland LR, Robinson V, Stratford IJ, Tozer GM, Watson S, Wedge SR, Eccles SA (2010) Guidelines for the welfare and use of animals in cancer research. *Br J Cancer* 102(11): 1555–1577

This work is published under the standard license to publish agreement. After 12 months the work will become freely available and the license terms will switch to a Creative Commons Attribution-NonCommercial-Share Alike 3.0 Unported License.